# Statistical mechanics of fluids adsorbed in planar wedges: Finite contact angle

J. R. Henderson
*School of Physics and Astronomy, University of Leeds, Leeds LS2 9JT, United Kingdom*
(Received 25 February 2004; published 23 June 2004)

I consider the statistical mechanics of inhomogeneous fluids applied to fluids adsorbed in planar wedges. Exact results are described that belong to an infinite subset of models defined as the intersection of any two identical semi-infinite planar wall-fluid potentials. This geometry is interesting as a generic example of adsorption onto structured interfaces and of interfacial phase transitions controlled by the substrate geometry. Previously described virial theorems are extended to the case of a general wall-fluid model. This enables the consideration of wedge filling when Young's contact angle far from the wedge apex is finite. The virial theorems generate two important relations: the wedge sum rules. The first sum rule links the interfacial free energy far from the wedge apex to the structure induced at the apex. The second sum rule links the free energy of the apex region to the structure induced by the apex. When Young's contact angle at the wedge walls is finite these relations further yield an exact result for the macroscopic contact angle in terms of the nanoscopic structure at the three-phase contact line (the intersection of the liquid-vapor surface with a wedge wall): the contact angle sum rule. These exact results are of direct relevance to computer simulation studies of adsorbed films. In addition, they take on special significance in the vicinity of continuous interfacial phase transitions: an approach to complete filling and the filling transition at bulk liquid-vapor coexistence.

DOI: 10.1103/PhysRevE.69.061613 PACS number(s): 68.08.Bc, 68.43.−h, 68.03.Cd

## I. INTRODUCTION

The equilibrium statistical mechanics of inhomogeneous fluids has largely been developed in semi-infinite planar geometry [1,2]. Recent advances in technology have created an interest in extending this exact knowledge to liquid films adsorbed on substrates that are structured on the nano, meso and macro scales. This paper argues that models of fluids adsorbed in a planar wedge can usefully be regarded as a generic class of structured inhomogeneous fluids. Previous work has concentrated on hard-wall boundary conditions, where the relevance of geometry is particularly clear [3,4]. In Secs. II and III below I consider the generalization to standard models of wall-fluid interfaces, such as square-well fluid at a square-well wall, or Lennard-Jones fluid at a 9-3 or 10-4-3 wall. Colloidal systems are also relevant, due to the depletion attraction between colloidal particles and a wall. Section II considers the virial route of statistical mechanics, applied to systems where one of the boundary walls is grooved in a series of macroscopic planar wedges. The physical relevance of such a model is discussed in some detail, with emphasis on the attractive interactions arising from the wedge walls. With certain provisos, one arrives at generalizations of exact results previously derived for hard-wall boundary conditions, that hereinafter are referred to as the wedge sum rules (Sec. III).

Parry, Rascon, and Wood, in particular, have emphasized that wedge geometry introduces classes of interfacial phase transitions, intimately linked with wetting transitions at a semi-infinite planar wall [5,6]. This leads to interfacial critical phenomena partly controlled by the geometric parameters defining the structured surface: in particular, the approach to complete filling of a wedge, from off bulk liquid-vapor coexistence, and the associated filling transition at liquid-vapor coexistence. The presence of these interfacial phase transitions allows for arbitrary control over the amount of adsorbed fluid. It is here that the key significance of the attractive wall-fluid interactions arises. Namely, a wedge can be filled with a mesoscopic or macroscopic amount of liquid, even though far from the apex the wedge walls are not wet by liquid, [7,8]. This arises provided Young's contact angle $\theta$ with the wedge walls is finite. In theory the wedge can then be partly filled by saturated liquid by reducing the opening angle of the wedge ($\beta$) towards the value at which the liquid-vapor surface lies completely flat across the wedge: $\beta=\pi-2\theta$. At this special wedge angle a macroscopic planar wedge can adsorb an arbitrary but finite amount of saturated liquid, while maintaining mechanical equilibrium, the so-called filling condition. For more acute wedges the amount of liquid adsorbed in the wedge can be controlled by increasing the vapor pressure towards saturation; known as an approach to complete filling. If the system is kept at liquid-vapor coexistence and a thermodynamic quantity controlling $\theta$, such as temperature $T$, or alternatively the geometric quantity $\beta$ is varied, so that the filling condition is reached, then the system undergoes an interfacial phase transition known as the filling transition. Theory implies that the filling transition will often be a continuous phase transition, even though the wetting transition at $\theta=0_+$ would normally be first order [5].

From the physical existence of the continuous approach to complete filling at a finite contact angle (or a continuous filling transition) it follows that one can use the statistical mechanics of fluid adsorbed in a planar wedge as an alternative route to modeling the classical capillarity of three-phase coexistence and Young's contact angle. In Sec. IV below I show that this approach has the interesting advantage in providing virial theorems for the macroscopic Young's contact angle. Section V focuses on the filling transition itself, assuming it to be continuous, in the context of virial theorems. Both Secs. IV and V are outcomes of the explicit consider-

 

ation of attractive wall-fluid interactions. Hard-wall boundary conditions cannot be associated with a contact angle at the wedge walls less than $\pi$, because at liquid-vapor coexistence a planar hard wall is completely dry (i.e., the interface between a hard wall and saturated liquid consists of a macroscopic film of vapor). Thus hard-wall boundary conditions can only be used to discuss the approach to complete emptying at $\theta=\pi$, which is essentially equivalent to approaching filling in real systems when $\theta=0$.

## II. VIRIAL THEOREMS FOR WEDGE GEOMETRY

Virial theorems in classical statistical mechanics are generated by enclosing a many-body system with boundary walls and then considering the changes in free-energy arising from an infinitesimal translation of one or more of the walls. Since the total free energy of the system is stationary at equilibrium, at linear order the work done on the fluid by the walls must be equal and opposite to the work done on the walls by the fluid. Exact sum rules arise provided one can usefully partition these two classes of work, although this can sometimes be far from straightforward in practice [9]. Virial theorems therefore come in complementary pairs, whereby the intermolecular interactions and correlations appearing in a theorem either belong to the fluid-wall interface or to the fluid region far from the boundary that has been moved. One can transform between these equivalent sum rules by integrating the condition for mechanical equilibrium across the boundary wall [10].

Let us now consider a standard virial analysis for the system sketched in Fig. 1. Only the right-hand boundary will be moved as part of the virial process, along the $x$ direction. The left-hand boundary is not drawn nor considered below because the system is taken to be macroscopic so that there are no fluid-mediated interactions between bulk fluid (at $x_b$) and the right-hand wall. Similarly, there are no interactions between the inhomogeneous fluid regions at macroscopically separated sections of the walls. The right-hand wall in Fig. 1 has a geometry such that it creates three identical planar wedges of opening angle $\beta$. Two of these wedges involve the horizontal planar walls at the top and bottom of the system, which will be taken to be identical to the walls forming the right-hand wedge. Due to the two-dimensional symmetry we can take $L_y \to \infty$ first, which is equivalent to ignoring the $\beta=\pi/2$ side wedges. For any given wedge, we can regard the position of a relevant wedge wall to be defined by a linear function $x_w(z)$. The walls drawn in Fig. 1 and below represent the surface of infinite repulsion between the one-body external field $v^{\text{ext}}(\mathbf{r})$ that defines any wall-fluid model and the centers of the fluid molecules; in particular, this bounds the volume $V$ accessible to the centers of the molecules. As I shall discuss in Sec. III, it is implicit that all iso-potential surfaces defined by $v^{\text{ext}}(\mathbf{r})$, such as attractive wall-fluid interactions, possess the identical wedge geometry of the repulsive boundary.

To derive the desired virial theorem consider an infinitesimal change in the value of $L_x$, which is equivalent to a translation of that part of $v^{\text{ext}}(\mathbf{r})$ associated with the far-right boundary only:

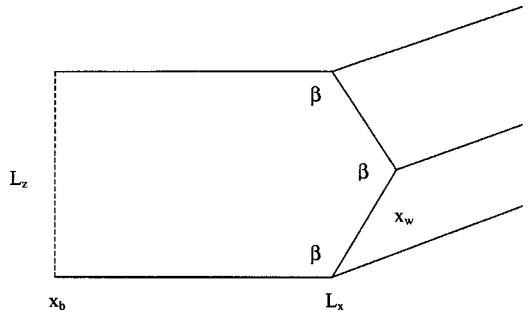


FIG. 1. System geometry used for the derivation of virial theorems for fluids in a planar wedge. Here, I have chosen one example of a planar wedge structure to the right-hand boundary of the system. For this example, the construction generates three identical planar wedges each of opening angle $\beta=2\pi/3$. The quantity $x_w$ denotes the position of this right-hand boundary wall. For rigorous derivations, any system should be fully enclosed by containing walls. To aid the reader with imagining the figure as forming part of the boundary of a three-dimensional box (with a structured right-hand wall) I have sketched the right-hand boundary in three dimensions and drawn part of a side wall lying in the $xz$ plane. Only the right-hand wall of this box is structured, so that the top and bottom walls (lying in the $xy$ plane) are planar rectangles (not fully drawn). Note that, apart from the three wedges whose opening angles are labeled $\beta$, all the remaining intersections between adjacent walls generate right-angled wedges ($\beta=\pi/2$). The dashed line denotes a distance from the right-hand boundary at which the presence of the $\beta=2\pi/3$ wedges is no longer felt. I have not drawn the left-hand boundary nor additional sidewalls because these play no role in the subsequent derivations. In the thermodynamic limit, all of the statistical mechanics derived in this paper applies to fluid adsorbed in a single wedge defined as the intersection of two identical semi-infinite planar walls, at an arbitrary value of $\beta$.

$$\frac{\partial v^{\text{ext}}((x-L_x),y,z)}{\partial L_x} = -\frac{\partial v^{\text{ext}}((x-L_x),y,z)}{\partial x}. \tag{1}$$

An important wedge sum rule then follows from the virial theorem [2]

$$\frac{\partial \Omega}{\partial L_x} = \int d\mathbf{r}\rho(\mathbf{r})\frac{\partial v^{\text{ext}}(\mathbf{r})}{\partial L_x} \tag{2}$$

$$= -\int_0^{L_y} dy \int_0^{L_z} dz \int_{x_b}^{\infty} dx \rho(\mathbf{r}) \nabla^x v^{\text{ext}}(\mathbf{r}) \tag{3}$$

$$= -\int_0^{L_y} dy \int_0^{L_z} dz p_T(y,z;x=x_b). \tag{4}$$

Here I have taken the free energy to be the fluid Grand potential $\Omega$. The Grand ensemble is the usual ensemble applied to inhomogeneous fluids since they are typically defined as subsystems in equilibrium with bulk fluid. The derivation of Eq. (3) from Eq. (2) has used Eq. (1). The step from Eq. (3) to Eq. (4) is much bigger and involves the condition for mechanical equilibrium (or equivalently the conservation of momentum) in the form [11]

$$-\rho(\mathbf{r})\nabla^x v^{\text{ext}}(\mathbf{r}) = kT\nabla^x\rho(\mathbf{r}) + \langle\sum_i \delta(\mathbf{r}-\mathbf{r}_i)\nabla_i^x\Phi\rangle, \quad (5)$$

where $k$ denotes Boltzmann's constant and the total system Hamiltonian is $H \equiv \Phi + \Sigma_i\, v^{\text{ext}}(\mathbf{r}_i)$. Integrating the expression (5) leads to the general form

$$\int_{x_b}^{\infty} dx\rho(\mathbf{r})\nabla^x v^{\text{ext}}(\mathbf{r})$$

$$= kT\rho(x_b,y,z) - \int_{x_b}^{\infty} dx\langle\sum_i \delta(\mathbf{r}-\mathbf{r}_i)\nabla_i^x\Phi\rangle \quad (6)$$

$$\equiv kT\rho(x_b,y,z) - \int_{x_b}^{\infty} dx\nabla^\beta p_c^{x\beta}(\mathbf{r}), \quad (7)$$

where the final line has introduced the configurational contribution to the pressure tensor (note the use of the summation convention to imply that $\beta$ is summed over $x,y,z$). When Eq. (7) is introduced into Eq. (3) the off-diagonal terms in the pressure tensor ($\beta = y,z$) do not contribute. Thus, the final integral in Eq. (3) can be replaced by

$$kT\rho(x_b,y,z) + p_c^{xx}(y,z;x=x_b) \equiv p_T(y,z;x=x_b), \quad (8)$$

where the subscript $T$ denotes the transverse component of a pressure tensor; i.e., transverse to the planar walls of Fig. 1 in the vicinity of $x=x_b$, [11]. In the Appendix below, I present for completeness an explicit derivation of the above formalism for pair potential models.

From Eq. (4) we obtain precisely the anticipated form for the work done on the fluid due to the virial procedure

$$\frac{\partial\Omega}{\partial L_x} = -pL_yL_z + \int_0^{L_y} dy\int_0^{L_z} dz[p - p_T(y,z;x=x_b)] \quad (9)$$

$$= -pL_yL_z + 2\gamma(L_y+L_z), \quad (10)$$

where $p$ denotes the bulk fluid pressure and $\gamma$ is the wall-fluid surface tension of the planar wall-fluid interfaces at $x=x_b$. That is, when $L_x$ is scaled by an infinitesimal amount the changes to the system depicted in Fig. 1 involve a change in volume, a change in the surface areas of the planar side walls and a change in the length of the right-angled wedges running along the sides [note that I have neglected this final higher-order contribution on the right of Eq. (10)]. All of these changes can be regarded as occurring macroscopically to the left of the right-hand wall in Fig. 1, because this latter interfacial region is completely unchanged by a different choice of $L_x$. Accordingly, the virial theorem has yielded a sum rule for the surface tension of the planar regions of the wall-fluid interface. In the form of Eq. (9) it is just the well-known virial expression [1], while in the complementary form (3) the planar surface tension is defined in terms of the wall-fluid interfacial structure in the apex regions of the wedges on the right side of Fig. 1. It is, of course, this latter version that we shall now focus attention on.

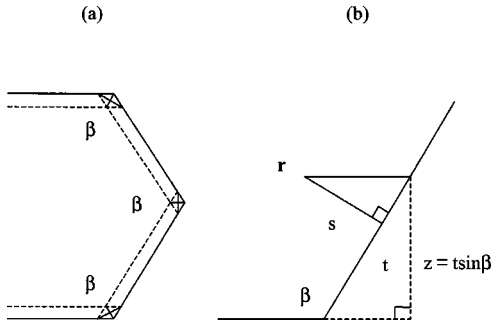


FIG. 2. (a) Profile of the right-hand wall in Fig. 1, illustrating (i.e., not drawn to scale) the significance of iso potentials of the attractive part of the wall-fluid interaction (dashed lines). Each planar section of wall generates planar iso potentials defined by a semi-infinite wall-fluid potential. The crossed regions, deep in the apexes of the wedges, denote positions at which adsorbed molecules feel attractions from both adjoining walls (up to the iso potentials depicted). This has been done simply to draw attention to the fact that the full wedge model is the sum of the two wall-fluid interactions acting on the apex regions. (b) Coordinate system used to denote a molecular center positioned a distance $t$ from a wedge wall, along the other wall, at a distance $s$ from the infinite wall-fluid repulsion boundary of the wall of interest.

## III. WEDGE SUM RULES

There are two main applications of the sum rules discussed below. In the first case we can imagine the wedge completely full of fluid, so that one is concerned with the molecular scale structure of fluids confined in a wedge, as could readily be studied by computer simulation procedures. In the second class of application we can use the presence of interfacial phase transitions to apply the sum rules to mesoscopic or macroscopic interfaces arising from two-phase coexistence within the wedge. In the latter case, the molecular scale structure at the extreme apex of the wedge is of no consequence. However, in the former case the results will be dependent on the detailed molecular structure assumed by the Hamiltonian (external field). Thus, let us first consider the physical relevance of a wedge model when attractive wall-fluid interactions are to be included.

Figure 2(a) depicts an iso-potential of the attractive part of the wall-fluid interaction energy. I shall define a planar wedge model to be restricted to this geometry; namely, all iso potentials must possess an identical wedge shape. Without such a restriction, the apex region of a wedge (crossed regions) would be highly model dependent and different iso potentials would typically possess different geometries. For the restricted class of model, the wedge model, one can introduce the coordinate system of Fig. 2(b). In particular, I can associate an ensemble-averaged wall force per unit area (pressure) with a distance $t$ from the apex of a wedge

$$\overline{p}(t) \equiv \int_{x_b}^{\infty} dx\rho(\mathbf{r})\nabla^x v^{\text{ext}}(\mathbf{r}) \quad (11)$$

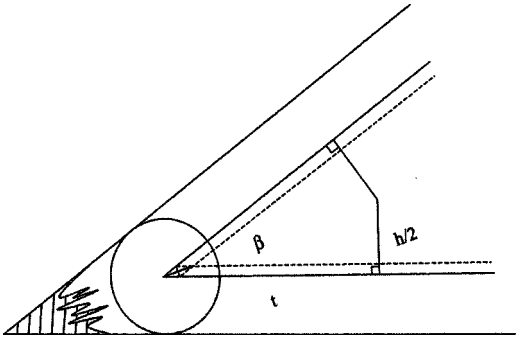


FIG. 3. An illustration of a planar wedge model applied to colloidal physics. A single colloidal sphere is depicted trapped at the apex of the wedge by the combination of depletion attractions with both walls (the crossed region at the apex).

$$= -\int_{-\infty}^{\infty} ds\rho(s,t)v'(s), \tag{12}$$

where the lower limit of the final integral is used to take full account of repulsive interactions (i.e., any hard-wall contribution [4]). That is, I have assumed a model such that the external field due to a single wedge wall is of the form $v^{\text{ext}}(\mathbf{r})=v(s)$ and the planar wedge geometry in the coordinate system of Figs. 1 and 2 has allowed for the change of variables $\rho(x,z)\to\rho(s,t)$. In some apex regions there are significant contributions from both adjoining walls; i.e., two integrals of the form (12), as discussed below in conjunction with Fig. 4. Figure 2(b) can be used to illustrate the nature of the integral (12); namely, the density profile is being sampled along a horizontal line (fixed $z$ and hence fixed $t$) with $s$, defined as the perpendicular to the containing boundary, varying accordingly. There is no Jacobian associated with the change of variables $x\to s$ because of the presence of the derivative in the integrand. With this notation, any choice of planar wall-fluid potential can be used in conjunction with the planar wedge model defined as the intersection of two semi-infinite planar walls. For example, consider a hard-wall repulsion ($hw$) together with a soft interaction or a square-well attraction ($att$)

$$v(s) = v_{\text{hw}}(s) + v_{\text{att}}(s). \tag{13}$$

For this class of model, Eq. (12) evaluates to

$$\overline{p}(t) = kT\rho_w(t) - \int_0^{\infty} ds\rho(s,t)v'_{\text{att}}(s) \tag{14}$$

$$\equiv kT\,[\rho_w(t) - \overline{\rho}_{\text{att}}(t)], \tag{15}$$

where $\rho_w(t)$ denotes the fluid density at the hard repulsive boundary and I have defined $\overline{\rho}_{\text{att}}$ because this quantity is particularly physical for a square-well model. An illustration of such a model applied to colloidal physics is shown in Fig. 3. Even in the absence of direct attractions the main effect of solvent-solute and solvent-wall repulsions is to induce a depletion attraction between colloidal particles with the walls and with each other [12]. Let us use Fig. 3 to consider the physical relevance of a planar wedge model. First, it is important to note that the wedge geometry belongs to the wall-fluid interaction (the inner wedge depicted in Fig. 3) and not necessarily the physical boundary (the outer boundary depicted in Fig. 3 including a jagged portion). Thus for colloidal experiments it would not be necessary to perfectly machine the apex region of the physical wedge, because this region is not part of the accessible phase space. For molecular fluids this remark is still relevant, but less dramatic. For acute wedges the fluid at one wedge wall is significantly influenced by the presence of the other wall, for distances $t$ from the wedge apex such that $h$ is less than a fluid correlation length. In this region, one would expect $\overline{p}(t)$ to be dominated by the confinement of the fluid in the wedge and a good approximation should be to set $\overline{p}(t)\to p(h)$ the solvation or disjoining pressure in a planar slit model at wall separation $h$, [3,12]. Beyond this region $\overline{p}(t)$ reduces to the bulk fluid pressure $p$; i.e., when $\rho(s,t)\to\rho(s)$ in Eq. (12). For molecular systems, the choice of wedge model is directly relevant to the fluid structure within a few molecular diameters of the apex of the wedge, given that nanoscience progresses sufficiently to be able to control such fine geometric detail and hence make this issue relevant. My choice of model (wedge shaped iso potentials) is fully consistent with, say, a square-well wall-fluid potential, but not with the strict physical basis of a 9-3 or 10-4-3 potential obtained by integration over a semi-infinite solid. In these cases the planar wedge model is double counting interactions coming from the complementary wedge shape reflected into the solid walls. Note that this issue is least significant for acute wedges and there is no link here with nanoscopic values of $h$ (which are associated with mesoscopic values of $t$ for very acute wedges).

We are now in position to be able to apply the virial route to the general planar wedge model. When the right-hand wall in Fig. 2(a) is moved, the virial theorem picks up contributions proportional to the integral of $\overline{p}(t)$ out from the apex of each wedge. Since only the right-hand wall is moved, there is only one such integral for each of the top and bottom wedges in Fig. 2(a), while in contrast there are two such contributions from the middle wedge, making a total of four. Note that by taking the thermodynamic limit the length of the wedge walls can be regarded as macroscopic and so each such integral can end half-way along a wall (denoted $\infty$ below) where $\overline{p}(t)=p$. The validity of the wedge sum rule obtained from this procedure depends on each of these four integrals being identical. This relies on the strict wedge-shaped iso potentials sketched in Fig. 2(a) together with the construction of Fig. 4. Note that Fig. 4(a) is relevant to the bottom wedge in Fig. 2(a), while Fig. 4(b) concerns the middle wedge. The virial procedure does not move the bottom wall in Fig. 4(a) because it is lying parallel to the $x$ axis. This issue is relevant to the crossed regions in Fig. 2(a), where the iso potentials of the attractive fields from adjoining wedges walls have overlapped. Given my interpretation of Fig. 4, one can construct any number of identical wedges out of the right-hand wall of Fig. 1 and so vary the wedge angle $\beta$, then equate the right side of Eq. (10) with the right side of Eq. (3). The latter generates a series of integrals over

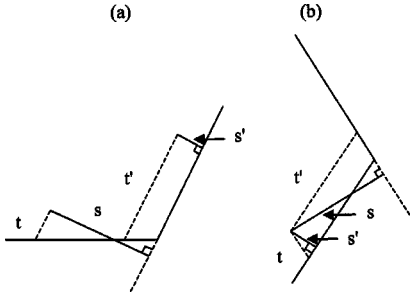


FIG. 4. Coordinate systems for the density profile $\rho(s,t)$ in a planar wedge model. (a) With respect to one wall only. Due to the wedge symmetry $\rho(s,t)=\rho(s',t')$. (b) With respect to both walls, a single point in space generates the values of $(s,t)$ and $(s',t')$ shown in (a). By symmetry there is an equivalent position on the other side of the wedge (not drawn).

$\overline{p}(t)$ multiplied by geometric factors needed to turn an integral over $dz$ into one over $dt$, such as sin $\beta$ in Fig. 2(b). The total sum of these integrals can be viewed as a phasor diagram such as the example of Fig. 5. For a detailed discussion of this geometric procedure applied to hard-wall models, including the trivial extension to include acute angled wedges, the reader is referred to Ref. [4]. In summary, the above virial procedure generates the important sum rule

$$\gamma = -\tan(\beta/2)\int_0^\infty dt[\overline{p}(t)-p]_\beta, \tag{16}$$

where the geometric prefactor has resulted from the phasor analysis and the integral runs from the apex of a wedge out along one of the planar sidewalls. Note that $\gamma$ denotes the interfacial free energy (surface tension) of the planar wall-fluid interface arbitrarily far from the apex.

There is a closely related sum rule, the second important wedge sum rule, that follows from the virial procedure

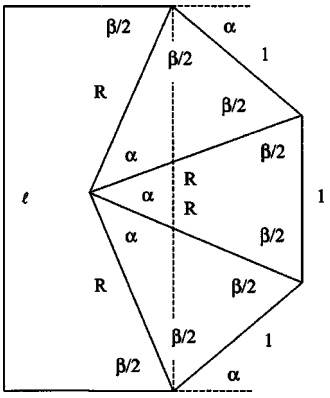


FIG. 5. Phasor diagram for the derivation of sum rule (16) at wedge angle $\beta > \pi/2$. The far right boundary is constructed from $n$ unit lengths that form a series of identical wedges of angle $\beta$, spanning an arc of angle $n\alpha$ and radius $R$. Here drawn for $n=3$ but $n$ could be any positive integer. From the $n+3$ sided polygon (solid outer boundary), whose angles must sum to $(n+1)\pi$, we have $\beta = n\pi/(n+1) = n\alpha$. From the vertical dashed line and any of the triangles it follows that $\ell = 2R\sin(\beta/2) = \tan(\beta/2)$.

whereby the wedge angle $\beta$ is varied; i.e., one of the walls is moved while pivoted to the apex. This process changes the fluid volume and the wedge angle, but not the surface area exposed to fluid ($2A$), and so generates a sum rule concerning the line tension (free-energy per unit length) $\tau$ of the wedge

$$\Omega \equiv -pV + 2\gamma A + \tau L_y. \tag{17}$$

It is straightforward to write down the general sum rule for $\partial\tau/\partial\beta$ [3]. However, as with the first wedge sum rule, it is not so straightforward to sort out the details of the model dependence in the apex region of the wedge. If we use Fig. 3 to visualize the virial process involved, it is clear that since only one of the wedge walls needs to be moved that the result can be expressed in terms of an integral along that wedge wall alone, just like sum rule (16). Provided all of the iso potentials defined by our wedge model possess the wedge shape drawn in Fig. 3, including the crossed region at the very apex (as if the iso potentials extended inside the solid walls), then the integrand should again be proportional to $[\overline{p}(t)-p]$. There will, however, be an extra power of $t$ in the integrand, due to the cylindrical coordinate system appropriate to the new virial procedure [3]. That is, we must use Fig. 2(b) in conjunction with the definition of $\overline{p}$ and invoke the same $(s,t)$ coordinate system, but now with $\partial s = t\partial\beta$ since all the iso potentials are rotated by the same angle $\partial\beta$. A sceptical, or confused, reader might prefer instead to consider a square-well wall model and directly evaluate Eq. (10) of Ref. [3]. I shall simply quote the general result whose validity depends on these subtle considerations:

$$\frac{\partial\tau}{\partial\beta} = -\int_0^\infty dtt[\overline{p}(t)-p]_\beta. \tag{18}$$

Again, let me stress that the hard part of the derivation is to understand the physical or molecular meaning of a wedge model at the level of the molecular detail assumed at the wedge apex. In the remainder of this paper I shall apply the above sum rules to mesoscopic/macroscopic issues in capillarity, making use of wedge geometry, where the validity of the wedge sum rules is on completely solid ground.

## IV. CONTACT ANGLE SUM RULE FROM THE APPROACH TO COMPLETE FILLING

If in the approach to bulk liquid-vapor coexistence (saturated vapor) a wedge apex becomes filled with a concave wedge of adsorbed liquid, as drawn in Fig. 6(a), then at saturation the wedge will be filled with a macroscopic amount of liquid even though the wedge walls are not completely wet by liquid. This corresponds to the condition $0<\theta<\psi$ where $\psi \equiv \pi/2-\beta/2$ is a complementary wedge angle and $\theta$ denotes Young's contact angle for a macroscopic drop of saturated liquid sitting in mechanical equilibrium on a semi-infinite planar surface (or arbitrarily far from the wedge apex). As the vapor pressure is increased towards saturation, the approach to complete filling of a wedge (as just defined) is a continuous process, an example of a continuous interfacial phase transition analogous to but separate

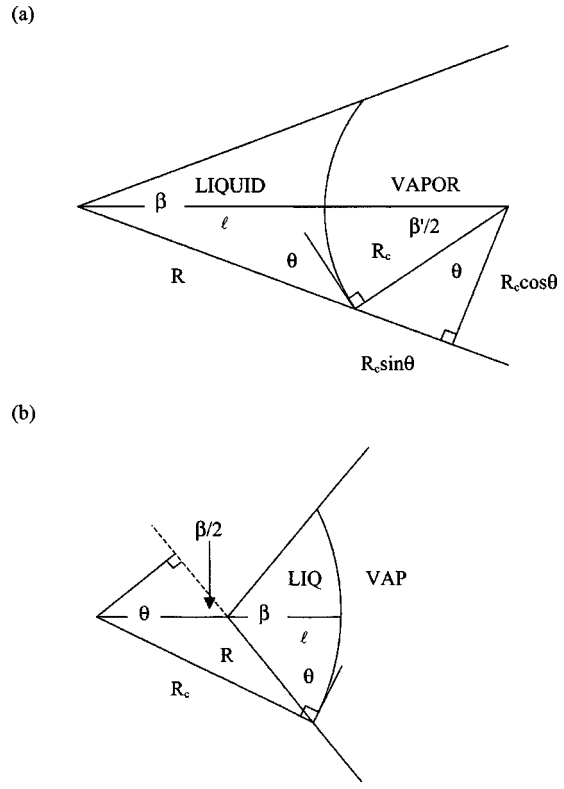


FIG. 6. Wedge geometry with mesoscopic/macroscopic amounts of adsorbed liquid, at finite Young's contact angle $\theta$. (a) $\theta<\psi \equiv \pi/2-\beta/2$, so that increasing the vapor pressure towards saturation leads to an approach to complete filling of a planar wedge. From the large right-angled triangle we have $\ell/R_c=(\cos\theta/\cos\psi)-1$ and $R/R_c=[\cos\theta/\tan(\beta/2)]-\sin\theta$. (b) Assuming the existence of a continuous filling transition at bulk saturation a mesoscopic amount of liquid has been adsorbed in the wedge at $\theta>\psi$. From the two right-angled triangles we have $\ell/R_c=1-(\cos\theta/\cos\psi)$ and $-R/R_c=[\cos\theta/\tan(\beta/2)]-\sin\theta$. If one redrew the diagram to apply to contact angles $\theta>\pi/2$ then the same geometric results are just as readily derived, but, of course, physically such a wedge would have to be dry in thermodynamic equilibrium. The boundary between wetting and drying of a wedge is $\theta=\pi/2$, or $\ell=R_c=R$ for any wedge angle.

from an approach to complete wetting at a planar surface (the latter occurs at $\theta=0$ only). On a semi-infinite planar surface an adsorbed drop at finite contact angle is not in thermodynamic equilibrium, since eventually the drop of excess liquid will evaporate to leave an adsorbed film of planar symmetry. In contrast, the picture sketched in Fig. 6(a) is in both thermodynamic and mechanical equilibrium. When the amount of adsorbed liquid $(\ell)$ is mesoscopic/macroscopic then the influence of the apex region no longer extends to the three-phase contact line that intersects the wedge walls at $t=R$. The angle $\theta$ is then Young's contact angle (in full equilibrium) and mechanical equilibrium can be expressed as Laplace's equation for the macroscopic pressure difference $\Delta p \equiv p_L - p_V$, across the liquid-vapor interface, in terms of its radius of curvature $R_c$; i.e., $\Delta p=-\gamma_{\rm LV}/R_c$. Wedge geometry is therefore an alternative and in some ways superior approach to classical capillarity [13,14], for which we now possess two powerful sum rules.

Consider the system depicted in Fig. 6(a) when all the lengths specified in the diagram are mesoscopic/macroscopic. The surface tension appearing on the left side of sum rule (16) is the wall-fluid interfacial free energy, per unit area, arbitrarily far from the wedge apex $(t=\infty)$; i.e., $\gamma=\gamma_{\rm SV}$. Introducing the thermodynamic definition of Young's contact angle and applying sum rule (16) therefore implies

$$\gamma_{\rm SV}=\gamma_{\rm SL}+\gamma_{\rm LV}\cos\theta \tag{19}$$

$$=-\tan(\beta/2)\left\{\int_0^R dt[\overline{p}(t)-p_L+\Delta p]_\beta + \int_{R_-}^{R_+} dt[\overline{p}(t)-p]\right\} \tag{20}$$

$$=\gamma_{\rm SL}-R\Delta p\tan(\beta/2)-\tan(\beta/2)\int_{R_-}^{R_+} dt[\overline{p}(t)-p]. \tag{21}$$

Here the notation is such that the interval $R_-<t<R_+$ covers the nanoscopic range over which the SLV contact line intersects (influences) the otherwise planar wall-fluid interfacial structure at $t\approx R$. Note that in this final integral in Eqs. (20) and (21) and below, I do not label the bulk pressure $p$ with a subscript, although outside the range $R_-<t<R_+$ one must, of course, take $p=p_V$. This highlights the fact that the integral is formally defined for a macroscopic system (where the difference between the saturated pressure $p$ and the vapor pressure $p_V$ has gone to zero). Any correction to this limit would be at the level of the curvature correction to $\gamma_{\rm LV}$; Tolman's length [1,2]. Similarly, there is no subscript $\beta$ on the integrand because the integral now belongs to a semi-infinite system. Accordingly, from this particular application of the wedge sum rule, we are led to a third important sum rule, this time for Young's contact angle. Namely, when Laplace's equation is used to eliminate $\Delta p$ and $R/R_c$ is evaluated as in the caption to Fig. 6(a), one obtains by equating Eq. (19) with Eq. (21) the following virial theorem for Young's contact angle:

$$\gamma_{\rm LV}\sin\theta=-\int_{R_-}^{R_+} dt[\overline{p}(t)-p]. \tag{22}$$

This remarkable result belongs to the same class of sum rules as Eq. (15) and hence also the famous prototype $p=kT\rho_w$ relating the bulk pressure to the density profile at a planar hard wall. In hindsight the result (22) is obvious because $\gamma_{\rm LV}\sin\theta$ is the component of the liquid-vapor surface tension acting normal to the surface of the planar wall. An interesting aspect of the sum rule is that by construction Young's contact angle is a mesoscopic/macroscopic quantity formally defined by structure arbitrarily far from the three-phase contact line, whereas the integrand on the right side of sum rule (22) is nonzero only in a nanoscopic region defined by the intersection of the range of the wall-fluid interaction and the area over which the fluid density profile is influenced by the intersection with the three-phase contact line. For ex-

ample, for a standard square-well model this is restricted to lie within half a molecular diameter from the repulsive boundary. Thus, if there currently exists any doubt among readers as to whether such a sum rule defines Young's contact angle or instead some ill-defined microscopic contact angle present *at* the interface, then the above derivation has fully confirmed the former interpretation. This conclusion is totally consistent with the structure of all wall-fluid virial theorems, as discussed in Sec. II, which always relates properties defined by macroscopic thermodynamics (deep inside the system) to structure present at the boundaries of the system. In the case of sum rule (22) this structure is the deformation by the three-phase contact line of the density profile, that would otherwise be fully defined by the force generated by the wall.

We are now presented with the interesting challenge that the virial theorem for Young's contact angle must be equally consistent with the second wedge sum rule Eq. (18). Confirmation requires us to first identify the line tension $\tau$ for the situation depicted in Fig. 6(a). This follows by treating the equimolar dividing surface of the liquid-vapor interface (extrapolated to the walls) and the wedge-shaped walls of infinite wall-fluid repulsion as Gibbs dividing surfaces, in order to define the excess wedge free-energy per unit length or line tension $\tau$, through the following decomposition of the fluid Grand potential:

$$\Omega = \Omega_{\rm SL}(V_L, A_{\rm SL}, L_y) + \Omega_{\rm SV}(V - V_L, A - A_{\rm SL}) + \gamma_{\rm LV} A_{\rm LV} + 2\tau_{\rm SLV} L_y \tag{23}$$

$$= -p_L V_L + 2\gamma_{\rm SL} A_{\rm SL} + \tau_{\rm SL} L_y - p_V[V - V_L] + 2\gamma_{\rm SV}[A - A_{\rm SL}] + \gamma_{\rm LV} A_{\rm LV} + 2\tau_{\rm SLV} L_y \tag{24}$$

$$= -p_V V + 2\gamma_{\rm SV} A - \Delta p V_L - 2(\gamma_{\rm SV} - \gamma_{\rm SL}) A_{\rm SL} + \gamma_{\rm LV} A_{\rm LV} + (\tau_{\rm SL} + 2\tau_{\rm SLV}) L_y \tag{25}$$

$$\equiv -p_V V + 2\gamma_{\rm SV} A + \tau L_y. \tag{26}$$

In these equations $A_{\rm SL}$ denotes that part of the area of each wall that is wet by liquid ($t < R$). There are three line tension contributions: $\tau_{\rm SLV}$ is the line tension of the three-phase contact line, $\tau_{\rm SL}$ is the line tension at the apex of the wedge (the only contribution if the wedge was completely filled with liquid), while the third, fourth and fifth terms on the right side of Eq. (25) arise from volume and area contributions due to the presence of two-phase coexistence in the wedge. Inserting Laplace's equation and Young's Eq. (19) into Eq. (25) and equating with Eq. (26) we have

$$\tau - \tau_{\rm SL} - 2\tau_{\rm SLV} = \gamma_{\rm LV}\left\{\frac{1}{R_c}\frac{V_L}{L_y} - 2\cos\theta\,\frac{A_{\rm SL}}{L_y} + \frac{A_{\rm LV}}{L_y}\right\} \tag{27}$$

$$= \gamma_{\rm LV}\{(R\cos\theta - \beta' R_c/2) - 2R\cos\theta + \beta' R_c\} \tag{28}$$

$$= -\gamma_{\rm LV} R_c\left\{\frac{R\cos\theta}{R_c} + \frac{\beta}{2} + \theta - \frac{\pi}{2}\right\}, \tag{29}$$

where the volumes and areas have been evaluated from Fig. 6(a). The three-phase contact line tension is independent of the wedge angle $\beta$ so it is only $\tau_{\rm SL}$ and the combination of the two-phase coexistence terms that enter into sum rule (18). That is, the wedge angle derivative is carried out at a fixed bulk thermodynamic state, fixed temperature $T$ and chemical potential $\mu$ (or vapor pressure $p_V$), so that $\tau_{\rm SLV}$, $\theta$, $\gamma_{\rm LV}$, and $R_c$ are all held fixed. Therefore, calculating the derivative of $R/R_c$ as given in the caption to Fig. 6(a), the left side of sum rule (18) evaluates to

$$\frac{\partial \tau}{\partial \beta} = \frac{\partial \tau_{\rm SL}}{\partial \beta} + \frac{\gamma_{\rm LV} R_c}{2}\left\{\frac{\cos^2\theta}{\sin^2(\beta/2)} - 1\right\}. \tag{30}$$

In the situation depicted in Fig. 6(a) the right side of sum rule (18) evaluates to

$$-\int_0^R dt t[\overline{p}(t) - p_L + \Delta p]_\beta - R\int_{R_-}^{R_+} dt[\overline{p}(t) - p] = \frac{\partial \tau_{\rm SL}}{\partial \beta} - \frac{R^2 \Delta p}{2} + R\gamma_{\rm LV}\sin\theta, \tag{31}$$

where in the final term I have substituted sum rule (22). Consistency between all three sum rules therefore requires the last few terms in Eqs. (30) and (31) to be equal. This final step follows by substituting Laplace's equation for $\Delta p$:

$$\frac{\partial \Delta\tau}{\partial \beta} = \frac{\gamma_{\rm LV} R_c}{2}\left\{\left(\frac{R}{R_c}\right)^2 + 2\frac{R}{R_c}\sin\theta\right\} \tag{32}$$

$$= \frac{\gamma_{\rm LV} R_c}{2}\left\{\frac{\cos^2\theta}{\tan^2(\beta/2)} - \sin^2\theta\right\} \tag{33}$$

$$= \frac{\gamma_{\rm LV} R_c}{2}\left\{\frac{\cos^2\theta}{\sin^2(\beta/2)} - 1\right\}. \tag{34}$$

Note that here I have defined $\Delta\tau \equiv \tau - \tau_{\rm SL} - 2\tau_{\rm SLV}$, which is the line tension arising from the presence of macroscopic liquid-vapor coexistence in the wedge. The only other contribution to $\partial\tau/\partial\beta$ arises from $\tau_{\rm SL}$, which is the apex line tension discussed in the previous section; i.e., arising from the region $t$ and $h$ both less than a liquid state correlation length (see Fig. 3).

## V. FILLING TRANSITIONS

The quantity $\Delta\tau$ defined in the previous section is the free energy per unit length controlling interfacial phase transitions associated with planar wedge geometry. For example, in the situation depicted in Fig. 6(a) we have $\ell/R_c = (\cos\theta/\cos\psi) - 1$ and so if the system approaches saturation at fixed $T$ and finite contact angle $\theta < \psi$ it follows that singular behavior can only arise from $R_c$; i.e., $\ell \sim R_c$. Since $-\gamma_{\rm LV}/R_c = \Delta p \to \Delta\rho\delta\mu$ it follows that $\ell \sim |\delta\mu|^{-1}$ in the approach to complete filling from off two-phase coexistence ($\delta\mu = 0$) [14]. The special situation $\theta = \psi$ yields an empty

wedge (no macroscopic filling) except at saturation. At bulk liquid-vapor coexistence higher-order terms in $\ell/R_c$ (typically beyond geometry, such as dispersion interactions) can theoretically lead to a mesoscopic/macroscopic amount of filling along a path $\theta \to \psi$ from above. Experimentally one would envisage changing $T$ and $\mu$ along the bulk coexistence curve to let $\theta$ approach $\psi$ at fixed geometry, but in terms of the singular behavior this is mathematically equivalent to varying the wedge angle so that $\psi$ approaches a fixed $\theta > 0$ (i.e., at fixed $T, \mu$). If the amount of liquid in the wedge were to diverge continuously along either of these paths in phase space, then one would observe the critical filling transition predicted by Parry, Rascon, and Wood [5,6]. The purpose of this section is to note that sum rule (18) is immediately applicable to critical filling at fixed temperature and chemical potential.

First, however, we need to extend our analysis of the wedge angle sum rule to the case $\theta > \psi$, where complete filling is absent at saturation. From Fig. 6(b) we see that the only difference with our analysis above is that $\Delta p$ has changed sign. In turn, this means that the derivation leading to Eq. (34) goes through unchanged, apart from a minus sign appearing on the right side. Introducing the amount of filling $\ell$ and the complementary wedge angle $\psi$, as in the caption to Fig. 6 so that in particular $\sin(\beta/2) = \cos\ \psi$, one finds that for all values of $\theta$ sum rule (18) can be written as

$$\frac{\partial \Delta\tau}{\partial \beta} = \frac{\gamma_{\mathrm{LV}}\ell}{2}\left(\frac{\cos\ \theta}{\cos\ \psi} + 1\right). \tag{35}$$

At filling, defined by $\theta = \psi$, where the liquid-vapor interface has a macroscopic curvature of precisely zero, this sum rule reduces to the simple result

$$\frac{\partial \Delta\tau}{\partial \beta} = \gamma_{\mathrm{LV}}\ell. \tag{36}$$

The physical interpretation of this special case is that the torque $\partial\Delta\tau/\partial\beta$ arises entirely from the stretching or compression of a flat liquid-vapor interface of area $2R\ \sin(\beta/2)L_y$; i.e., at $\theta = \psi$ the wedge geometry reduces to $R\ \cos(\beta/2) = R\ \sin\ \theta = \ell$.

The significance of the exact result (36) to critical filling is that it implies an amplitude relation and a critical exponent relation, since the singular contribution to the free energy must be contained in $\Delta\tau$. Writing

$$\Delta\tau = A_\tau(\delta\beta)^{2-\alpha_w}, \quad \ell = A_\ell(\delta\beta)^{-\beta_w}, \tag{37}$$

where $\delta\beta \equiv \beta - \pi + 2\theta$, it follows from the sum rule (36) that

$$\frac{A_\tau}{A_\ell} = \frac{\gamma_{\mathrm{LV}}}{(2-\alpha_w)}, \quad 1 - \alpha_w = -\beta_w. \tag{38}$$

Exactly the same exponent relation applies to an approach to complete wetting at a planar interface (see, e.g., Ref. [2]), however, Parry and co-workers have shown that the manner in which this exponent relation is satisfied for critical filling is far more complicated. In fact, the main correspondence (or covariance) is with critical wetting at a planar surface (especially in strong fluctuation regimes) except that both $d$ and $d-1$ dimensional exponents, or contributions to the exponents, are present [5,6].

## VI. DISCUSSION

In this paper I have derived three important sum rules that constrain the structure and free energy of fluids adsorbed in planar wedges and at the planar walls. The first sum rule links the interfacial free energy far from the wedge apex to the structure induced at the apex. The second sum rule links the free energy of the apex region to the structure induced by the apex. The generality of these results hinges on whether or not one can usefully define a general class of wedge models. I argued that requiring all iso potentials of the wall-fluid potential to possess planar wedge geometry is a sufficient criterion for any such model to satisfy the wedge sum rules. Of course, given the complexity of the details involved with Fig. 4 it would be helpful to confirm this conclusion with computer simulation procedures applied to a model of the class defined in this paper. I have also noted a warning that, in general, this strict adherence to wedge symmetry deep within the apex region will not always be a truly realistic model of an experimental system, at the molecular level. Notwithstanding this caveat, it is important to develop models of structured substrates that allow for attractive wall-fluid interactions, as proposed in this work. Alternative classes of models will satisfy analogous virial theorems for the same physical reasons, derivable by similar procedures, but the simplicity of the final forms might have to be sacrificed.

In Secs. IV and V above I have made use of planar wedge geometry to consider, from this different perspective, the statistical mechanics of classical capillarity. Because of the presence of complete filling in a wedge at finite values of Young's contact angle, it is physically possible to ensure mesoscopic or macroscopic two-phase coexistence within a wedge. In this situation, the details of the molecular structure at the wedge apex become irrelevant and the wedge sum rules describe the classical capillarity associated with Laplace and Young. In particular, both sum rules yield a virial theorem for Young's contact angle. This final result links the macroscopic contact angle and the liquid-vapor surface tension, defined arbitrarily far from the wedge walls, to the distortion of the density profile within the range of the wall potential due to the intersection of the three-phase contact line with the wedge walls. From the derivation of the contact angle virial theorem it follows that it is an expression of mechanical force balance normal to the interface and as such is the twin to Young's Eq. (19) expressing force balance parallel to the interface. When expressed in this context, it is clear that the contact angle virial theorem will have been addressed in one form or another many times before. The value of a wall-fluid model is that the normal force due to the wall can be trivially expressed in terms of a one-body density profile and the external (wall) field. This important interpretation does not appear have been appreciated before. In particular, sum rule (22) allows for the calculation of an interfacial free energy directly from an average over one-body structure. Typically, such a dramatic improvement in computational efficiency is associated with the derivative of a free

energy (an order parameter) rather than with the free energy itself. This has arisen because, as with the prototype hard-wall result $p=kT\rho_w$, the sum rule was derived from virial theorems in which the thermodynamic field derivative is with respect to a geometric quantity defining the system size, and so the associated order parameter is an intensive free energy. Finally, I have applied sum rule (18) to critical filling transitions. Given the physical existence of a critical filling transition, the line tension must contain a singular contribution as a function of wedge angle. This wedge sum rule therefore contains important information about interfacial critical phenomena in wedge geometry.

The study of adsorption in planar wedges is of relevance to other realizations of the wetting of structured substrates. Annular wedges, such as formed in the surface forces apparatus, will display analogous physics. The sum rules derived in this paper are of immediate value to computer simulation procedures, which can simulate the identical class of models, but the associated physics is of direct relevance to experiments and technology based on microstructured or nanostructured substrates. The virial theorem for Young's contact angle would appear to have wide significance to classical capillarity, as an exact realization of contact angle phenomena and as a direct route to calculating interfacial free energies from one-body structure.


## ACKNOWLEDGMENT

It is a pleasure to thank A. O. Parry for extensive discussion and correspondence on the nature of filling transitions.


## APPENDIX: PAIR POTENTIAL MODELS

For a pair potential model we write

$$\Phi = \frac{1}{2}\sum_i \sum_{j\neq i} \phi(r_{ij}). \tag{A1}$$

The final term in Eq. (5), the general expression of mechanical equilibrium, then evaluates to

$$\left\langle \sum_i \delta(\mathbf{r}-\mathbf{r}_i)\nabla_i^x \Phi \right\rangle = -\left\langle \sum_i \sum_{j\neq i} \delta(\mathbf{r}-\mathbf{r}_i)(x_j-x_i)\frac{\phi'(r_{ij})}{r_{ij}} \right\rangle \tag{A2}$$

$$= -\int d\mathbf{r}_2 \rho^{(2)}(\mathbf{r}_1,\mathbf{r}_2)(x_2-x_1)\frac{\phi'(r_{12})}{r_{12}}\bigg|_{\mathbf{r}_1=\mathbf{r}}. \tag{A3}$$

The final term in Eq. (7) is therefore

$$\int_{x_b}^{\infty} dx_1 \int_0^{x_b} dx_2 \int_0^{L_y} dy_2 \int_0^{L_z} dz_2 \rho^{(2)}(\mathbf{r}_1,\mathbf{r}_2)(x_2-x_1)\frac{\phi'(r_{12})}{r_{12}}$$
$$= -\frac{1}{2}\int_{-\infty}^{\infty} dx_{12} x_{12}^2 \int_0^{L_y} dy_2 \int_0^{L_z} dz_2 \rho^{(2)}(\mathbf{r}_1,\mathbf{r}_2)\frac{\phi'(r_{12})}{r_{12}}, \tag{A4}$$

where I have made use of the symmetry of the integrand to write the left-hand side and the short-ranged nature of the integrand to obtain the right-hand side. So, dropping the unwanted contributions from the side walls at $y=0, L_y$, the right side of Eq. (7) for a pair potential model is

$$kT\rho(z) - \frac{1}{2}\int_{-\infty}^{\infty} dx_{12} \int_{-\infty}^{\infty} dy_{12} \int_0^{L_z} dz_2 \times \rho^{(2)}(r_{12},z,z_2) x_{12}^2 \frac{\phi'(r_{12})}{r_{12}}, \tag{A5}$$

which is the transverse component of the pressure tensors of Harasima and Kirkwood and Buff [1,11]. That is, the integrand of Eq. (4) is precisely the form expected.


[1] J. S. Rowlinson and B. Widom, *Molecular Theory of Capillarity* (Clarendon, Oxford, 1982).
[2] J. R. Henderson, *Fundamentals of Inhomogeneous Fluids*, edited by D. Henderson (Dekker, New York, 1992), Chap. 2.
[3] J. R. Henderson, Physica A **305**, 381 (2002).
[4] J. R. Henderson, J. Chem. Phys. **120**, 1535 (2004).
[5] A. O. Parry, C. Rascon, and A. J. Wood, Phys. Rev. Lett. **85**, 345 (2000); A. O. Parry, A. J. Wood, and C. Rascon, J. Phys.: Condens. Matter **13**, 4591 (2001).
[6] A. O. Parry, C. Rascon, and A. J. Wood, Phys. Rev. Lett. **83**, 5535 (1999); A. O. Parry, A. J. Wood, and C. Rascon, J. Phys.: Condens. Matter **12**, 7671 (2000); A. O. Parry, M. J. Greenall, and A. J. Wood, *ibid.* **14**, 1169 (2002); M. J. Greenall, A. O. Parry, and J. M. Romero-Enrique, preprint (2004).
[7] R. Shuttleworth and G. L. J. Bailey, Discuss. Faraday Soc. **3**, 16 (1948).
[8] P. Concus and R. Finn, Proc. Natl. Acad. Sci. U.S.A. **63**, 292 (1969).
[9] J. R. Henderson, J. Phys.: Condens. Matter **11**, 629 (1999).
[10] M. M. Bakri, Physica (Amsterdam) **32**, 97 (1966); this apparently forgotten early work contains a general analysis relevant to my Sec. II, but readers should beware that the final section has not withstood the test of time. A similar approach was presented much later by M. J. P. Nijmeijer and J. M. J. van Leeuwen, J. Phys. A **23**, 4211 (1990).
[11] See, for example, P. Schofield and J. R. Henderson, Proc. R. Soc. London, Ser. A **379**, 231 (1982).
[12] For a review of the statistical mechanics of depletion interactions see J. R. Henderson, Physica A **313**, 321 (2002).
[13] Y. Pomeau, J. Colloid Interface Sci. **113**, 5 (1986).
[14] E. H. Hauge, Phys. Rev. A **46**, 4994 (1992).